Thermodynamic Assessment of the Mn-B System

Weihua Sun, Yong Du, Shuhong Liu, Baiyun Huang, and Chao Jiang

(Submitted October 16, 2009; in revised form January 17, 2010)

The phase equilibrium and thermodynamic data on the Mn-B system are critically reviewed. Based on the experimental data, a thermodynamic modeling is performed on this system. A set of self-consistent thermodynamic parameters is obtained and the calculated results are in general agreement with the experimental data. A parameter ξ is introduced to compare the degree of flatness of the δMn/L liquidus with those in other metal-boron systems. It is found that the δMn/ L liquidus is the flattest, which causes difficulties in its modeling. An effective approach to evaluate the thermodynamic parameters for o-$Mn_2B_{0.982}$ phase is developed. Such an approach is valid for evaluating thermodynamic parameters of the phases with limited phase diagram data.

1. Introduction

Boron and manganese are useful alloying elements that can improve the strength of many metal (e.g., Al, Cu, Fe, and Ni) based materials. In order to construct a thermodynamic database for those materials, a thermodynamic assessment on the Mn-B subsystem is necessary. The Mn-B system has been assessed by four groups of researchers.[1-4] Among them, Liao and Spear[3] have made a critical literature review and thermodynamic modeling on this system. However, a thermodynamic reassessment of the Mn-B system is still meaningful for the following reasons. First, more accurate lattice stabilities[5] for the pure elements are available. Second, when using the parameters from Liao and Spear,[3] the calculated phase diagram shows two miscibility gaps associated with liquid phase, as shown in Fig. 1. Finally, new partial enthalpy of mixing for the liquid phase has been measured by Vitusevich.[6] The purpose of this study is to critically review the literature data and provide a set of self-consistent thermodynamic parameters for the Mn-B system by means of the CALculation of PHAse Diagrams (CALPHAD) approach.

Weihua Sun and **Chao Jiang**, State Key Laboratory of Powder Metallurgy, Central South University, Changsha, Hunan 410083, China; **Yong Du, Shuhong Liu,** and **Baiyun Huang**, State Key Laboratory of Powder Metallurgy, Central South University, Changsha, Hunan 410083, China and Science Center for Phase Diagram & Materials Design and Manufacture, Central South University, Changsha, Hunan 410083, China. Contact e-mail: yongduyong@ gmail.com.

2. Literature Review

2.1 Phase Diagram Data

In order to facilitate reading, the crystal structure data on all the phases reported in the literature are listed in Table 1. By using a combination of X-ray diffraction (XRD), thermal analysis (TA), chemical analysis, and metallographic observation, Markovskii and Bezruk[7-11] made a comprehensive investigation on the phase equilibria and proposed a whole Mn-B phase diagram.[11] Six compounds were reported: Mn_4B, t-Mn_2B, MnB, Mn_3B_4, MnB_2, and MnB_4. Although all of these compounds were confirmed to exist, most of the equilibrium data reported by Markovskii and Bezruk[11] were updated by subsequent researchers.[12-23] In the following, the phase relationship in the Mn-B phase diagram is critically discussed.

In the range from MnB_2 to pure B, Markovskii and Bezruk[11] reported two eutectic reactions: L ↔ MnB_2 + MnB_4 at 1800 °C and L ↔ MnB_4 + β(B) at 1880 °C. In addition, MnB_2 was determined to have a large homogeneity range. α(B) was found to be stable at low temperature with a transformation to β(B) at 1300 °C. However, MnB_4 was confirmed to decompose into MnB_2 and β(B) at high temperature.[13,16,17,20,22,23] Andersson and Carlsson[17] reported the decomposition temperature to be between 1350 and 1400 °C. In addition, MnB_2 decomposes to Mn_3B_4 and MnB_4[13,14,16,17,20,22,23] at lower temperature. The decomposition temperature determined by Andersson and Carlsson[17] was between 1050 and 1100 °C, which was consistent with the result of Cely et al.[20] who reported the temperature to be between 1050 and 1150 °C. The homogeneity range of MnB_2 was very narrow.[15,20] Moreover, the phases in the MnB_x (x > 2) alloy after melting were MnB_2 and β(B),[16,17,20] which also indicates that an eutectic reaction L ↔ MnB_2 + β(B) exists rather than L ↔ MnB_2 + MnB_4 or L ↔ MnB_4 + β(B).

In the composition range from MnB to MnB_2, the invariant reactions reported by Markovskii and Bezruk[11] were L ↔ MnB + Mn_3B_4 and MnB_2 + L ↔ Mn_3B_4. However, the experimental results of Hoyle[22] showed that the
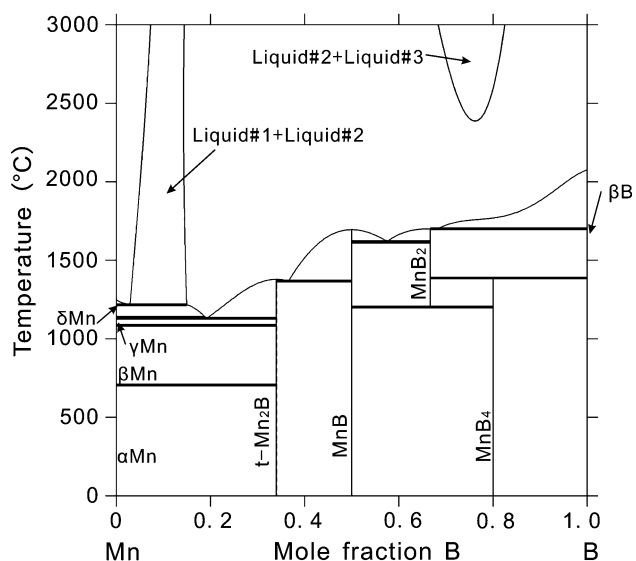
Fig. 1 Calculated Mn-B phase diagram according to the parameters from Liao and Spear.[3] It should be mentioned that the Gibbs energies for pure elements are obtained from Dinsdale[5] since these data used by Liao and Spear[3] are not available. Such a treatment causes the calculated phase diagram differs with that from Liao and Spear.[3] However, we just address the miscibility gaps of the liquid phase, which are only relevant with the interaction parameters for liquid phase rather than the Gibbs energies for pure elements

invariant reactions in this region are $MnB + L \leftrightarrow Mn_3B_4$ and $L \leftrightarrow Mn_3B_4 + MnB_2$. The experimental evidences from Hoyle[22] were adopted in the assessed Mn-B phase diagram[3,4] and were also accepted in the present modeling.

In the range from $t-Mn_2B$ to MnB, the only experimental investigation is due to Markovskii and Bezruk.[11] Therefore, the phase equilibria reported by them[11] were adopted in both the assessed phase diagram[3,4] and the present modeling.

In the composition range from pure Mn to $t-Mn_2B$, Markovskii and Bezruk[11] reported two reactions: $L \leftrightarrow Mn_4B + \alpha(Mn)$ at 1180 °C and $L + t-Mn_2B \leftrightarrow Mn_4B$ at 1285 °C. However, $\alpha(Mn)$ cannot be stable above 727 °C.[5] By means of chemical analysis, XRD, differential thermal analysis (DTA), and microscopy, Pradelli and Gianoglio[19] reinvestigated this part of the phase diagram and proposed an eutectic reaction ($L \leftrightarrow \delta Mn + t-Mn_2B$ at 1211 °C) and a peritectoid reaction ($Mn_4B \leftrightarrow \gamma Mn + t-Mn_2B$ at 1124 °C). In addition, Mn_4B has a large homogeneity range from 20 to 33.3 at.% B.[19] Later, Mn_4B was refined to be $o-Mn_2B$ with orthorhombic structure.[21] The composition of $o-Mn_2B$ was actually determined to be $o-Mn_2B_{0.982}$ when considering the occupancy of boron position.[21] Since the data reported by Pradelli and Gianoglio[19] were self-consistent, they were adopted in the assessed phase diagram[3,4] and the present modeling.

Andersson and Carlsson[17] reported the maximum solubility of Mn in β(B) to be 4.2 at.% at high temperature.

Table 1 List of symbols and crystallographic data of the phases in the Mn-B system

Symbol	Pearson symbol/Space group/ Prototype	Lattice parameters (Å)	Comments	References
Liquid	...	...	...	...
(δMn)	cI2 Im3m W	a = 3.0806	Pure Mn	Liao[3]
(γMn)	cF4 Fm3m Cu	a = 3.8624	Pure Mn	Liao[3]
(βMn)	cP20 P4₁32 βMn	a = 6.3152	Pure Mn	Liao[3]
(αMn)	cI58 I43m αMn	a = 8.9139	Pure Mn	Liao[3]
o-Mn₂B₀.₉₈₂	oF48 Fddd ...	a = 14.54 b = 7.291 c = 4.208	...	Liao[3]
t-Mn₂B	tI12 I4/mcm CuAl₂	a = 5.148 c = 4.208	...	Liao[3]
MnB	oP8 Pnma FeB	a = 5.56 b = 2.977 c = 4.145	...	Liao[3]
Mn₃B₄	oI14 Immm Ta₃B₄	a = 3.03 b = 12.86 c = 2.96	...	Liao[3]
MnB₂	hP3 P6/mmm AlB₂	a = 3.007 c = 3.037	...	Liao[3]
MnB₄	mC14 C2/m Ni₃Sn₄	a = 5.503 b = 5.369 β = 122.71 °C c = 2.949	...	Liao[3]
MnB₂₃	hR108 R-3m ...	a = 10.9907 c = 23.9964	βB solution	Liao[3]
βB	hR108 R3m ...	a = 10.925 b = 23.81	Pure B	Liao[3]
Mn₄Bᵃ	oF40 Fddd Mn₄B	a = 14.53 b = 7.293 c = 4.209	...	Liao[3]
αMnB	oC8 Cmcm CrB	...	...	Okamoto[4]
βMnB	oP8 Pnma FeB	...	...	Okamoto[4]

ᵃMn₄B and o-Mn₂B₀.₉₈₂ refer to the same phase

However, the temperature for the maximum solubility was not specified. As a result, the solubility of Mn in β(B) was considered to be 4.2 at.% at the eutectic temperature of the reaction L ↔ MnB$_2$ + β(B) in the present modeling.

Kiessling[12] reported that the solubility of B in (Mn) was negligible by XRD. However, Cely et al.[20] indicated that B could dissolve interstitially in (Mn), but did not give the solubility value. Since no significant solubility of B in (Mn) has been reported, the solubility was not considered in the present modeling.

For the MnB compound, Okamoto[4] reported that it has two structures. αMnB is stable at low temperature and transforms to βMnB at 1050 °C. However, in the measurement of the isothermal sections at 800 °C of Tm-Mn-B system by Chaban et al.[24] and Sc-Mn-B system by Mikhalenko et al.,[25] αMnB and βMnB were observed at 800 °C by XRD, respectively. Consequently, there is not sufficient evidence to demonstrate the stability of αMnB and βMnB for the moment. Thus, only one compound MnB was considered in the present modeling.

2.2 Thermodynamic Data

The partial enthalpies of Mn and B in liquid in the composition range from pure Mn to 52 at.% B at 1677 °C were measured by Esin et al.[26] using a high-temperature calorimeter. B with a low purity (98 wt.% B) was used in their study. Also, the wrong difference between the enthalpy of B at 0 °C and that at 1677 °C was used in their derivation for the partial enthalpy of B. With the same method as that employed by Esin et al.,[26] Vitusevich[6] measured the partial enthalpies of B and Mn in liquid at 1600 °C. The experimental data[6] were adopted by Vitusevich,[27-29] who critically evaluated the thermodynamic data of binary and ternary melts of the 3d transition metals (Cr, Mn, Fe, Co, and Ni) with B. Consequently, the experimental data from Vitusevich[6] were utilized in the present modeling. By solution calorimetry, Kleppa and Sato[30] determined the

enthalpies of formation of t-Mn$_2$B, MnB, and MnB$_2$ at 1113 °C, which were considered in the modeling.

The experimental data used in the optimization are listed in Table 2. Only the data from No. 1 to 11 were considered to be reliable as discussed above. In addition, since only Markovskii and Bezruk[11] have studied the phase equilibria in the composition range from t-Mn$_2$B to MnB, their reported phase equilibria data within this composition range were also used in the optimization. Other data from No. 13 to 16 were obtained from the assessed phase diagram due to Liao and Spear[3] since the temperatures for these reactions were not experimentally determined.

3. Thermodynamic Model

The Gibbs energy function $^0G_i^\varphi(T) = G_i^\varphi(T) - H_i^{SER}$ for the pure element i (i = Mn, B) is expressed as:

$$^0G_i^\varphi(T) = a + b \cdot T + c \cdot T \cdot \ln T + d \cdot T^2 + e \cdot T^{-1}$$
$$+ f \cdot T^3 + g \cdot T^7 + h \cdot T^{-9}, \qquad \text{(Eq 1)}$$

where H_i^{SER} is the molar enthalpy of the element i at 25 °C and 1 bar in its stable element reference (SER) state, and T is the absolute temperature. In the present modeling, the Gibbs energies as a function of temperature are taken from the SGTE compilation by Dinsdale.[5]

The Gibbs energy for φ (φ = liquid and β(B)) is described by the Redlich-Kister polynomial[31]:

$$G_m^\varphi - H^{SER} = (1-x) \cdot {}^0G_{Mn}^\varphi + x \cdot {}^0G_B^\varphi + R \cdot T \cdot$$
$$[(1-x) \cdot \ln(1-x) + x \cdot \ln x] + x \cdot (1-x)$$
$$[a_0 + b_0 \cdot T + (1-2x) \cdot (a_1 + b_1 \cdot T) + \cdots]$$
$$\text{(Eq 2)}$$

in which H^{SER} denotes $(1-x) \cdot H_{Mn}^{SER} + x \cdot H_B^{SER}$, R is the gas constant, and x represents the mole fraction of B. The

Table 2 List of the data used in the optimization

No	Experimental data	T (°C)	Ref.
1	Liquidus between liquid and δMn	...	[19]
2	Liquidus between liquid and t-Mn$_2$B	...	[19]
3	L ↔ δMn + t-Mn$_2$B	1211	[19]
4	o-Mn$_2$B$_{0.982}$ ↔ γMn + t-Mn$_2$B	1124	[19]
5	MnB + L ↔ Mn$_3$B$_4$	...	[22]
6	L ↔ Mn$_3$B$_4$ + MnB$_2$	...	[22]
7	L ↔ MnB$_2$ + β(B)	...	[16,17,20]
8	MnB$_2$ ↔ Mn$_3$B$_4$ + MnB$_4$	1050-1100	[17]
9	MnB$_4$ ↔ MnB$_2$ + β(B)	1350-1400	[17]
10	Partial enthalpy of mixing of liquid phase	1600	[27]
11	Enthalpy of formation of t-Mn$_2$B, MnB, MnB$_4$ (−31.7, −35.8, −21.1 kJ/mol ·atoms, respectively)	1113	[31]
12	Phase equilibria in t-Mn$_2$B to MnB part	...	[11]
13	MnB + L ↔ Mn$_3$B$_4$	1827	[3]
14	L ↔ Mn$_3$B$_4$ + MnB$_2$	1750	[3]
15	L ↔ MnB$_2$	1827	[3]
16	L ↔ MnB$_2$ + β(B)	1730	[3]

Table 3 Optimized thermodynamic parameters in the Mn-B system

Liquid: $(B, Mn)_1$
$^0L_{B,Mn}^L = -134141.3 - 15.7142 \cdot T$
$^1L_{B,Mn}^L = 32025.1 - 21.7659 \cdot T$
$^2L_{B,Mn}^L = 59907.4$
$^3L_{B,Mn}^L = -8723.6$

o-Mn$_2$B$_{0.982}$: $Mn_{0.670691}B_{0.329309}$
$^0G_{Mn:B}^{o-Mn_2B_{0.982}} - 0.670691 \cdot {}^0G_{Mn}^{\alpha Mn} - 0.329309 \cdot {}^0G_B^{\beta B} = -31651.9 - 6.17 \cdot T$

t-Mn$_2$B: $Mn_{0.666667}B_{0.333333}$
$^0G_{Mn:B}^{t-Mn_2B} - 0.666667 \cdot {}^0G_{Mn}^{\alpha Mn} - 0.333333 \cdot {}^0G_B^{\beta B} = -31700 - 6.4802 \cdot T$

MnB: $Mn_{0.5}B_{0.5}$
$^0G_{Mn:B}^{MnB} - 0.5 \cdot {}^0G_{Mn}^{\alpha Mn} - 0.5 \cdot {}^0G_B^{\beta B} = -35800 - 9.9995 \cdot T$

Mn$_3$B$_4$: $Mn_{0.428571}B_{0.571429}$
$^0G_{Mn:B}^{Mn_3B_4} - 0.428571 \cdot {}^0G_{Mn}^{\alpha Mn} - 0.571429 \cdot {}^0G_B^{\beta B} = -38786.7 - 6.9904 \cdot T$

MnB$_2$: $Mn_{0.333333}B_{0.666667}$
$^0G_{Mn:B}^{MnB_2} - 0.333333 \cdot {}^0G_{Mn}^{\alpha Mn} - 0.666667 \cdot {}^0G_B^{\beta B} = -21100 - 12.556 \cdot T$

MnB$_4$: $Mn_{0.2}B_{0.8}$
$^0G_{Mn:B}^{MnB_4} - 0.2 \cdot {}^0G_{Mn}^{\alpha Mn} - 0.8 \cdot {}^0G_B^{\beta B} = -17744.3 - 4.5934 \cdot T$

βB: $(B, Mn)_1$
$^0G_B^{\beta B} = GHSERB$
$^0G_{Mn}^{\beta B} = GHSERMn + 40$
$^0L_{B,Mn}^{\beta B} = -49500 - 21 \cdot T$

αMn: $(Mn)_1(B, Va)_1$
$^0G_{Mn:Va}^{\alpha Mn} = GHSERMn$
$^0G_{Mn:B}^{\alpha Mn} = GHSERMn + GHSERB$

βMn: $(Mn)_1(B, Va)_1$
$^0G_{Mn:Va}^{\beta Mn} = GCUBMn$
$^0G_{Mn:B}^{\beta Mn} = GCUBMn + GHSERB$

γMn: $(Mn)_1(B, Va)_1$
$^0G_{Mn:Va}^{\gamma Mn} = GFCCMn$
$^0G_{Mn:B}^{\gamma Mn} = GFCCMn + GFCCB$

δMn: $(Mn)_1(B, Va)_3$
$^0G_{Mn:Va}^{\delta Mn} = GBCCMn$
$^0G_{Mn:B}^{\delta Mn} = GBCCMn + 3 \cdot GBCCB$

interaction coefficients a_j and b_j ($j = 0, 1, 2$) are to be evaluated in the optimization process.

The compounds o-Mn$_2$B$_{0.982}$, t-Mn$_2$B, MnB, Mn$_3$B$_4$, MnB$_2$, and MnB$_4$ are modeled as stoichiometric phases. The Gibbs energy for each compound is given by the following expression:

$$G(Mn_{(1-x)}B_x) - (1 - x) \cdot H_{Mn}^{SER} - x \cdot H_B^{SER}$$
$$= (1 - x) \cdot {}^0G_{Mn}^{\alpha Mn} + x \cdot {}^0G_B^{\beta B} + A + B \cdot T, \qquad \text{(Eq 3)}$$

where A and B are to be optimized.

The Gibbs energy for φ ($\varphi = \alpha Mn$, βMn, γMn, and δMn), is modeled by a two sublattice model $(Mn)_x(B, Va)_y$. Its Gibbs energy expression is expressed as follows:

$$G_{Mn:B,Va}^{\varphi} = (1 - y_B'') \cdot G_{Mn:Va}^{\varphi} + y_B'' \cdot G_{Mn:B}^{\varphi} +$$
$$R \cdot T \cdot [x \cdot (1 - y_B'') \cdot \ln(1 - y_B'') + y \cdot y_B'' \cdot \ln y_B'']$$
$$+ y_B'' \cdot (1 - y_B'')$$
$$\cdot [L_{Mn:B,Va}^0 + (1 - 2y_B'') \cdot L_{Mn:B,Va}^1 + \ldots] + {}^{mag}G_m$$
$$\text{(Eq 4)}$$

For αMn, βMn, and γMn, $x = y = 1$, for δMn, $x = 1$, $y = 3$. y_B'' represents the site fraction of B in the second sublattice. $L_{Mn:B,Va}^j$ ($j = 0, 1, 2$) denotes interaction between B and vacancy in the second sublattice. Since the solubility of B in (Mn) is not considered, $L_{Mn:B,Va}^j$ is not used.

The $^{mag}G_m$ term, which describes the magnetic contribution to the Gibbs energy, is given by the Hillert-Jarl-Inden model.[32,33] For δMn, γMn, and αMn phases, it is necessary to introduce $^{mag}G_m$ term, while for βMn phase, its $^{mag}G_m$ term is equal to zero.
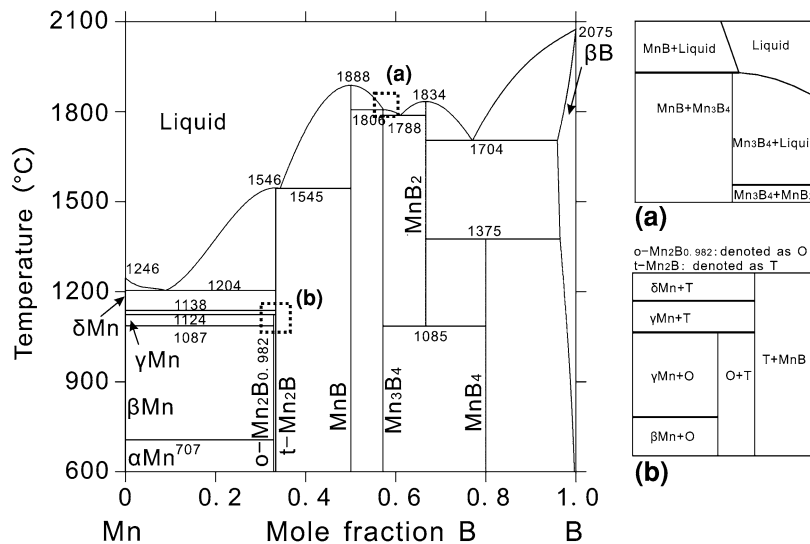

Fig. 2 Calculated Mn-B phase diagram according to the present modeling
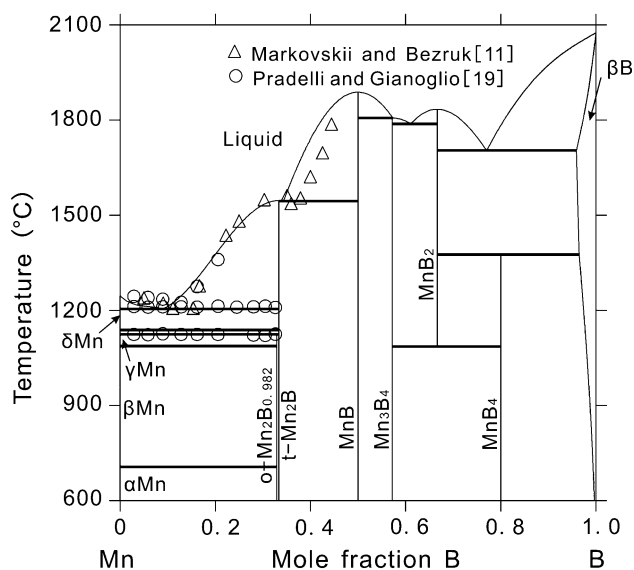
Fig. 3 Calculated Mn-B phase diagram with the experimental data[11,19]

4. Result and Discussion

The optimization began with the liquid phase. First, the parameters a_0 and a_1 for liquid phase could be optimized from the partial enthalpy of mixing.[6] Then, the optimization went to the Mn-MnB part and MnB-B part to adjust the parameters a and b for liquid phase and related compounds. As the solubility of Mn in β(B) is not appreciable, β(B) phase was considered later. Since o-Mn$_2$B$_{0.982}$ and MnB$_4$ were not connected with liquid phase and the parameters for these two compounds would not influence the previous optimized equilibria, they were considered at last. The optimized parameters for this system are listed in Table 3. The calculated phase diagrams with and without experimental data are shown in Fig. 2 and 3, respectively. Table 4 lists the invariant equilibria along with the measured[11,17,19] and assessed[3,4] equilibria. For the optimization procedure and result, six points need to be addressed.

First, since there is no experimental evidence to indicate that any or all compounds except MnB$_2$ will decompose at low temperature, an assumption that these compounds except MnB$_2$ are stable at 0 °C was made in the optimization.

Second, as shown in Table 3, $^0G_{Mn}^{\beta B} = GHSERMn + 40$ was introduced just to make $^0G_{Mn}^{\beta B}$ not influence the Mn boundary, and the solubility of Mn in β(B) was adjusted by the interaction parameter $^0L_{B,Mn}^{\beta B}$. Since there are no Gibbs energy functions for B with cub_A13 or cbcc_A12 structures, we use the approximation of $^0G_{Mn:B}^{\alpha Mn} = GHSERMn + GHSERB$ and $^0G_{Mn:B}^{\beta Mn} = GCUBMn + GHSERB$. Such a treatment does not cause any influence on the Mn rich region.

Third, the experimental δMn\L liquidus measured by Pradelli and Gianoglio[19] extends to 14.3 at.% B. However, the present modeling can only extend it to be 8.9 at.% B if

Table 4 Calculated invariant equilibria along with the measured[11,17,19] and assessed[3,4] equilibria in the Mn-B system

Reaction	Reference	Composition (at.% B)			T (°C)
L ↔ δMn + t-Mn$_2$B	This work	8.9	0	33.3	1204
	Pradelli[19]	14.3	<1	33.3	1211
	Liao[3]	15	0	33.3	1207
	Okamoto[4]	14.3	<1	33.3	1211
L ↔ t-Mn$_2$B	This work		33.3		1546
	Markovskii[11]		33.3		1580
	Liao[3]		33.3		1580
	Okamoto[4]		33.3		1580
L ↔ t-Mn$_2$B + MnB	This work	34.3	33.3	50	1545
	Markovskii[11]	...	33.3	50	1510
	Liao[3]	39	33.3	50	1510
	Okamoto[4]	37	33.3	50	1510
L ↔ MnB	This work		50		1888
	Markovskii[11]		50		1890
	Liao[3]		50		1890
	Okamoto[4]		50		1890
L + MnB ↔ Mn$_3$B$_4$	This work	57.3	50	57.1	1806
	Liao[3]	57.3	50	57.1	1827
	Okamoto[4]	...	50	57.1	1750
L ↔ Mn$_3$B$_4$ + MnB$_2$	This work	61.1	57.1	66.7	1788
	Liao[3]	61.5	57.1	66.7	1750
	Okamoto[4]	...	57.1	66.7	1630
L ↔ MnB$_2$	This work		66.7		1834
	Liao[3]		66.7		1827
	Okamoto[4]		66.7		1990
L ↔ MnB$_2$ + βB	This work	77	66.7	95.9	1704
	Liao[3]	80	66.7	100	1730
	Okamoto[4]	80	66.7	>95.5	1800
o-Mn$_2$B$_{0.982}$ ↔ γMn + t-Mn$_2$B	This work	32.9	0	33.3	1124
	Pradelli[19]	20-33	<1	33.3	1124
	Liao[3]	25	0	33.3	1120
MnB$_2$ ↔ Mn$_3$B$_4$ + MnB$_4$	This work	66.7	57.1	80	1085
	Andersson[17]	66.7	57.1	80	1050-1100
	Liao[3]	66.7	57.1	80	1100
	Okamoto[4]	66.7	57.1	80	1075
MnB$_4$ ↔ MnB$_2$ + βB	This work	80	66.7	96.5	1375
	Andersson[17]	80	66.7	...	1350-1400
	Liao[3]	80	66.7	100	1375
	Okamoto[4]	80	66.7	...	1375

the temperature for L ↔ δMn + t-Mn$_2$B is kept around 1211 °C. The δMn\L liquidus determined by Pradelli and Gianoglio[19] is very flat, which has been mentioned by Okamoto.[4] We compare the δMn\L liquidus with those in other systems[34,35] involving B by introducing a parameter ξ:

$$\xi = (T_m - T)/^L X_B \qquad (\text{Eq } 5)$$

where T_m is the melting point of an element M which is close to Mn in the Periodic table. T is the temperature of the eutectic reaction L ↔ M + M$_x$B$_y$. $^L X_B$ is the mole percent of B of liquid phase. The ξ for each system is listed in Table 5.

Table 5   Parameter $\xi = (T_m - T)/^L X_B$ in the M-B system

System (M-B)	T_m (°C)	Eutectic reaction	$^L X_B$ (at.% B)	T (°C)	$T_m - T$ (°C)	ξ
Mn-B	1246	$L \leftrightarrow \delta Mn + t\text{-}Mn_2B$	14.3	1211	35	2.4
Sc-B	1541	$L \leftrightarrow \beta Sc + ScB_2$	17	1277	264	15.5
Ti-B	1670	$L \leftrightarrow \beta Ti + TiB$	7	1540	130	18.6
V-B	1910	$L \leftrightarrow (V) + V_3B_2$	15	1735	175	11.7
Cr-B	1863	$L \leftrightarrow (Cr) + Cr_2B$	13.5	1630	233	17.3
Fe-B	1538	$L \leftrightarrow \gamma Fe + Fe_2B$	17	1174	364	21.4
Co-B	1495	$L \leftrightarrow \alpha Co + Co_3B$	18.5	1110	385	20.8
Ni-B	1455	$L \leftrightarrow (Ni) + Ni_3B$	17	1093	362	21.3
Cu-B	1085	$L \leftrightarrow (Cu) + B$	13.3	1013	72	5.4
Y-B	1522	$L \leftrightarrow \alpha Y + YB_2$	25.5	1290	232	9.1
Zr-B	1855	$L \leftrightarrow \beta Zr + ZrB_2$	13.7	1662	193	14.1
Nb-B	2469	$L \leftrightarrow (Nb) + Nb_3B_2$	14	1600	869	62.1
Mo-B	2623	$L \leftrightarrow (Mo) + Mo_2B$	23	2175	448	19.5

Fig. 4   Abnormal and normal $\delta Mn/L$ liquidus in the optimization

It can be clearly seen that ξ for the Mn-B system is significant smaller than that for any other system. This means that the Mn-rich liquidus in the Mn-B system is the flattest. In the optimization, the adjustment for the $\delta Mn \backslash L$ liquidus should be carried out very carefully. This flat liquidus tends to be not monotonic, as shown by the dashed line in Fig 4. Although the calculated liquidus from the previously parameters[3] can extend to 14.3% B, an abnormal liquid miscibility gap appears in the Mn-rich corner when using the Thermo-Calc S version or Pandat software. Since we keep the temperature for $L \leftrightarrow \delta Mn +$ t-Mn_2B around 1211 °C and make the $\delta Mn \backslash L$ liquidus monotonic as B content increases, the calculated eutectic composition at 8.9 at.% B instead of 14.3 at.% B can be accepted. Because there are no experimental data of greater reliability for this system, no attempt to use more parameters

for the adjustment of this liquidus was not considered since using more parameters is not encouraged by the CALPHAD optimization spirit.

Fourth, the parameters A and B for o-$Mn_2B_{0.982}$ were determined by the reaction o-$Mn_2B_{0.982} \leftrightarrow \gamma Mn +$ t-Mn_2B at 1124 °C and the limitation condition o-$Mn_2B_{0.982} \leftrightarrow \alpha Mn +$ t-Mn_2B and t-$Mn_2B \leftrightarrow$ o-$Mn_2B_{0.982} +$ MnB do not happen at 0 °C. They require that $-6.4113 < B < -6.1605$ and $A + B \cdot 1397.15 = -40272.2882$. The derivation of the relation is discussed in the following.

For o-$Mn_2B_{0.982} \leftrightarrow \gamma Mn +$ t-Mn_2B, we transform it to

$$2 \cdot o\text{-}Mn_2B_{0.982} = 0.072 \cdot \gamma Mn + 1.964 \cdot t\text{-}Mn_2B \quad \text{(Eq 6)}$$

If this reaction happens at T °C, we get

$$2 \cdot G(o\text{-}Mn_2B_{0.982}) = 0.072 \cdot G(\gamma Mn) \\ + 1.964 \cdot G(t\text{-}Mn_2B) \quad \text{at } T\,°C \quad \text{(Eq 7)}$$

When $T = 1124$ °C, $G(\gamma Mn)$ and $G(t\text{-}Mn_2B)$ are obtained from Dinsdale[5] and previous modeling, respectively. Inserting these values into Eq 7, we get

$$A + B \cdot 1397.15 = -40272.2882 \quad \text{(Eq 8)}$$

for the reaction o-$Mn_2B_{0.982} \leftrightarrow \gamma Mn +$ t-Mn_2B at 1124 °C.

Next, the limitation condition is considered. For o-$Mn_2B_{0.982} \leftrightarrow \alpha Mn +$ t-Mn_2B does not happen at 0 °C, we get

$$2 \cdot G(o\text{-}Mn_2B_{0.982}) < 0.072 \cdot G(\alpha Mn) + 1.964 \\ \cdot G(t\text{-}Mn_2B) \quad \text{at } 0\,°C \quad \text{(Eq 9)}$$

Similar as the derivation discussed above, we get

$$A + B \cdot 273.15 < -33066.0172 \quad \text{(Eq 10)}$$

Similarly, for t-$Mn_2B \leftrightarrow$ o-$Mn_2B_{0.982} +$ MnB does not happen at 0 °C, we get

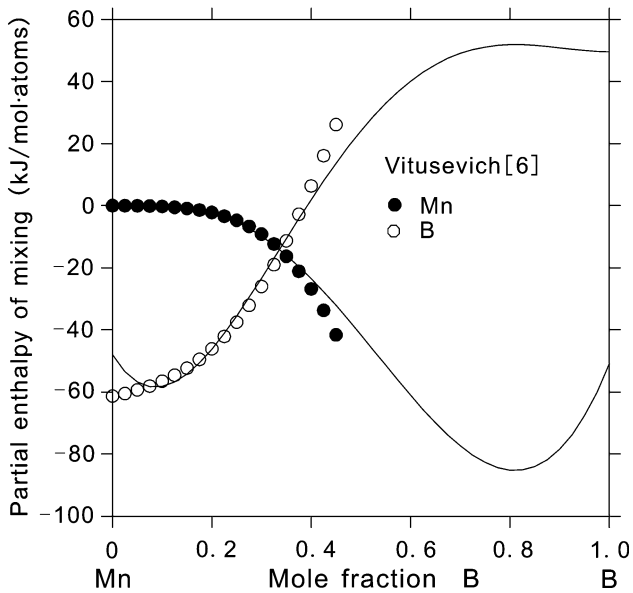$$A + B \cdot 273.15 > -33347.8623. \quad \text{(Eq 11)}$$

Fig. 5 Calculated partial enthalpies of mixing for Mn and B in liquid phase compared with the experimental data.[6] The reference states are liquid Mn and solid βB at 1600 °C

Fig. 6 Calculated enthalpy of formation compared with the experimental data.[30] The reference states are γMn and βB at 1113 °C

If we put Eq 8 into Eq 10 and 11, we get

$$-6.4113 < B < -6.1605 \qquad \text{(Eq 12)}$$

As a result, only if $A + B \cdot 1397.15 = -40272.2882$ with $-6.4113 < B < -6.1605$, o-Mn$_2$B$_{0.982}$ ↔ γMn + t-Mn$_2$B at 1124 °C and stabilities of o-Mn$_2$B$_{0.982}$ and t-Mn$_2$B at 0 °C can be satisfied.

Since there are groups of A and B for o-Mn$_2$B$_{0.982}$, we arbitrarily chose one group:

$$B = -6.17 \quad A = -31651.9$$

However, the parameters A and B for MnB$_2$ are fixed by MnB$_2$ ↔ Mn$_3$B$_4$ + MnB$_4$ and MnB$_4$ ↔ MnB$_2$ + βB. These two parameters should satisfy the limitation condition that MnB$_4$ ↔ βB + Mn$_3$B$_4$ and Mn$_3$B$_4$ ↔ MnB + MnB$_4$ do not happen at 0 °C. We attempted to make the MnB$_2$ ↔ Mn$_3$B$_4$ + MnB$_4$ and MnB$_4$ ↔ MnB$_2$ + βB to happen at 1075 and 1375 °C, respectively. However, they could not be satisfied completely at the same time because of the limitation condition. As a result, the MnB$_4$ ↔ MnB$_2$ + βB was adjusted to 1375 °C while MnB$_2$ ↔ Mn$_3$B$_4$ + MnB$_4$ was at 1085 °C.

Fifth, as shown in Fig. 3, the calculated phase diagram in the composition range from t-Mn$_2$B and MnB is not consistent with the experimental data from Markovskii and Bezruk.[11] In the optimization, it seems that it is impossible to completely reproduce the phase diagram data in the composition ranges from (Mn) to t-Mn$_2$B[19] and from t-Mn$_2$B to MnB.[11] In the assessment, more weight was given to the data in the range from (Mn) to t-Mn$_2$B.[19]

At last, the calculated thermodynamic properties are in good agreements with the experimental data[6,30] as shown in Fig. 5 and 6. The present calculated phase diagram is in
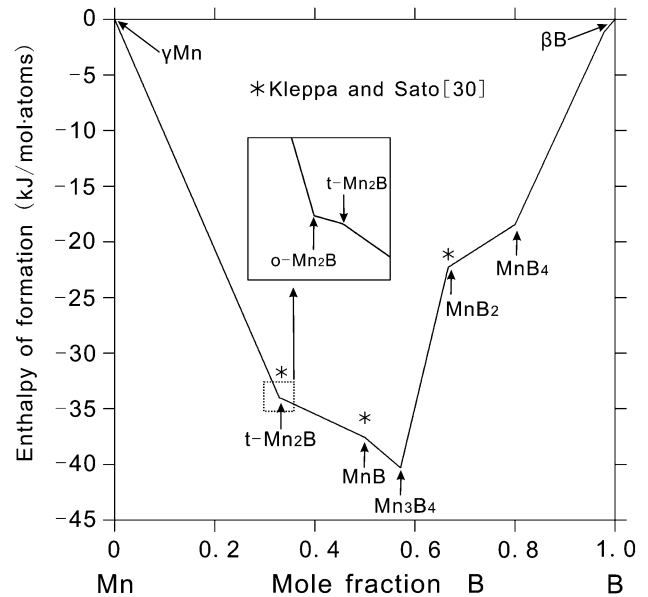
general agreement with the assessed phase diagram by Liao and Spear[3] as shown in Table 4. Although the temperatures for some invariant reactions show some differences from those in the assessed phase diagram by Okamoto,[4] all of calculated reaction types associated with the equilibria are the same as those assessed[3,4] or measured. Since some phase equilibria information used in the optimization was obtained from the assessed phase diagram by Liao and Spear,[3] additional experiments are needed.

5. Conclusion

- The Mn-B system is modeled based on critical literature review. A set of self-consistent parameters is obtained and the calculated results show general agreements with the reliable experimental data.
- The optimization procedure and results are critically discussed, particularly for the flat δMn/L liquidus, o-Mn$_2$B$_{0.982}$ and MnB$_4$. The δMn/L liquidus is determined to be the flattest when compared with the Metal/L liquidus in other systems. Such a flat liquidus makes modeling difficult. The ranges of the thermodynamic parameters for o-Mn$_2$B$_{0.982}$ are mathematically derived.
- More experimental work is needed to refine the present thermodynamic modeling.

References

1. K. Hack and T.G. Chart, Critical Assessment and Estimation of Thermodynamic Data for the Manganese-Boron System, *Comm. Eur. Commun.*, 1982, **7** (EUR 7820, Pt. 2), p 1-15

2. L. Kaufman, B. Uhrenius, D. Birnie, and K. Taylor, Coupled Pair Potential, Thermochemical and Phase Diagram Data for Transition Metal Binary Systems. VII, *Calphad*, 1984, **8**(1), p 25-66

3. P.K. Liao and K.E. Spear, The B-Mn (Boron-Manganese) System, *Bull. Alloy Phase Diag.*, 1986, **7**(6), p 543-549, p 585-586

4. H. Okamoto, B-Mn (Boron-Manganese), *J. Phase Equilib.*, 1993, **14**(1), p 121-122

5. A.T. Dinsdale, SGTE Data for Pure Elements, *Calphad*, 1991, **15**, p 317-425

6. V.T. Vitusevich, Enthalpy of Formation of Manganese-Boron-Carbon Melts, *Metally*, 1993, **4**, p 38-41, in Russian

7. L.Y. Markovskii and E.T. Bezruk, Melting Diagram and Some Properties of Borides in the Manganese Boron System, *Zh. Prikl. Khim.*, 1965, **38**(8), p 1677-1682, in Russian

8. L.Y. Markovskii and E.T. Bezruk, System Manganese-Boron, *Vysokotemp. Neorgan. Soedin., Akad. Nauk Ukr. SSR Inst. Probl. Materialoved*, 1965, p 433-436, in Russian

9. L.Y. Markovskii and E.T. Bezruk, Phase Composition of Compounds Forming in the Manganese-Boron Systems Rich in Boron, *Zh. Prikl. Khim.*, 1967, **40**(6), p 1199-1203, in Russian

10. E.T. Bezruk and L.Y. Markovskii, Lower Manganese Borides, *Zh. Prikl. Khim.*, 1967, **40**(4), p 908-911, in Russian

11. L.Y. Markovskii and E.T. Bezruk, Phase Diagram of the Manganese-Boron System, *Izv. Akad. Nauk SSSR, Neorg. Mater.*, 1967, **3**(12), p 2165-2169, in Russian

12. R. Kiessling, The Borides of Some Transition Elements, *Acta Chem. Scand.*, 1950, **4**, p 209-227

13. R. Fruchart and A. Michel, A New Boride of Manganese, MnB$_4$, *Compt. Rend.*, 1960, **251**, p 2953-2954, in French

14. I. Binder and B. Post, Manganese Diboride, *Acta Cryst.*, 1960, **13**, p 356-357

15. B. Aronsson, A Note on the Compositions and Crystal Structures of MnB$_2$, Mn$_3$Si, Mn$_5$Si$_3$, and FeSi$_2$, *Acta Chem. Scand.*, 1960, **14**(6), p 1414-1418

16. S. Andersson, A Note on the Crystal Structure of MnB$_4$, *Acta Chem. Scand.*, 1969, **23**(2), p 687-688

17. S. Andersson and J.-O. Carlsson, The Crystal Structure of MnB$_4$, *Acta Chem. Scand.*, 1970, **24**(5), p 1791-1799

18. S. Andersson and B. Callmer, The Solubilities of Copper and Manganese in β-Rhombohedral Boron as Determined in CuB$_{28}$ and MnB$_{23}$ by Single-Crystal Diffractometry, *J. Solid State Chem.*, 1974, **10**, p 219-231

19. G. Pradelli and C. Gianoglio, Manganese-Boron System, *Metall. Ital.*, 1974, **66**(12), p 659-662, in Italian

20. A. Cely, L.-E. Tergenius, and T. Lundstrom, Microhardness Measurements and Phase Analytical Studies in the Mn-B System, *J. Less-Common Met.*, 1978, **61**, p 193-198

21. L.E. Tergenius, Refinement of the Crystal Structure of Orthorhombic Mn$_2$B (Formerly Denoted Mn$_4$B), *J. Less-Common Met.*, 1981, **82**, p 335-340

22. S.Q. Hoyle, "The Phase Equilibria of the Mn-B System," Thesis, The Pennsylvania State University, University Park, Pennsylvania, May, 1981

23. R.T. Miller, "Manganese-Boron Phase Equilibria," Thesis, The Pennsylvania State University, University Park, Pennsylvania, May, 1982

24. N.F. Chaban, S.I. Mikhalenko, Y.Z. Kernitska, and Y.B. Kuz'ma, The Equilibrium Phase Diagram for the Tm-Mn-B System, *Powder Metall. Met. Ceram.*, 2001, **40**(5-6), p 258-261

25. S.I. Mikhalenko, V.S. Babizhets'kii, and Y.B. Kuz'ma, The Sc-Mn-B System, *Powder Metall. Met. Ceram.*, 2005, **44**(11-12), p 567-572

26. Y.O. Esin, V.M. Baev, and P.V. Gel'd, Enthalpies of Formation of Molten Manganese-Boron Alloys, *Zh. Fiz. Khim.*, 1975, **49**(11), p 2966-2967

27. V.T. Vitusevich, Thermodynamic Properties of Liquid Alloys of 3d Transition Metals with Metalloids (Silicon, Carbon and Boron), *J. Alloys Compd.*, 1994, **203**(1-2), p 103-110

28. V.T. Vitusevich, Thermodynamics of Binary and Ternary Melts of the 3d Transition Metals (Cr, Mn, Fe, Co and Ni) with Boron, *Thermochim. Acta*, 1995, **264**, p 41-58

29. V.T. Vitusevich, Thermodynamics of Liquid Binary Alloys of the 3d Transition Metals with Metalloids: Generalization, *J. Alloys Compd.*, 1995, **221**(1-2), p 74-85

30. O.J. Kleppa and S. Sato, New Applications of High-Temperature Solution Calorimetry. III. Enthalpies of Formation of Dimanganese Boride, Manganese Boride, and Manganese Diboride, *J. Chem. Thermodyn.*, 1982, **14**(2), p 133-143

31. O. Redlich and A. Kister, Thermodynamics of Nonelectrolytic Solutions. Algebraic Representation of Thermodynamic Properties and the Classification of Solutions, *Ind. Eng. Chem.*, 1948, **40**, p 345-348

32. G. Inden, *The Proceedings of CALPHAD V Project Meeting*, Max-Planck Institute for Metal Research, Dusseldorf, 1976, p 1-13

33. M. Hillert and M. Jarl, A model for alloying effects in ferromagnetic metals, *Calphad*, 1978, **2**(3), p 227-238

34. T.B. Massalski, J.L. Murray, L.H. Bennett, and H. Baker, Ed., *Binary Alloy Phase Diagrams*, Vol 1, 1st ed., ASM, Metals Park, OH, 1987, p 347-399

35. P.K. Liao and K.E. Spear, The B-Y (Boron-Yttrium) System, *J. Phase Equilib.*, 1995, **16**(6), p 521-524